Southeast Europe Journal of Soft Computing ISSN 2233 – 1859
Available online: http://scjournal.ius.edu.ba

Vol 12, No. 2, September 2023, pp. 78-87

Chemically radiative dissipative MHD Casson nanofluid flow on a non-linear elongating stretched sheet with numerous slip and convective boundary conditions

[1*]Mohammed Sarfaraz Hussain and [1]S Mohammed Ibrahim

[1]Research Scholar, Department of Engineering Mathematics,
College of Engineering, Koneru Lakshmaiah Education Foundation,
Vaddeswaram, Andhra Pradesh, 522302,,
Indiaa
**Corresponding Author*: ibrahimsvu@gmail.com

sarfaraz.maths@gmail.com

Article Info

Article history:

Article received on 09 10 2023

Received in revised form 01 11 2023

Keywords:

Stagnation point; Slip conditions; Casson nanofluid; Radiation; Chemical reaction; MHD.

ABSTRACT: The flow of a Casson nanofluid across a nonlinear stretching surface with a velocity slip and a convective boundary condition is investigated in this work in the magnetohydrodynamic (MHD) domain. This technique emphasizes a variety of effects, including chemical reaction, viscosity dissipation, and velocity ratio.

In this study, Brownian motion and thermophoresis are also illustrated. It is assumed that suction exists while a magnetic field is uniform. The governing nonlinear partial differential equations are converted into a set of nonlinear ordinary differential equations using the required similarity transformations, and the Runge-Kutta-Fehlberg fourth-fifth method is then used to solve the system. The updated results are fairly similar to the earlier ones. The graphs and tables examine how various variables affect the speeds, temperatures, concentrations of substances, skin friction values, Sherwood numbers and Nusselt numbers.

1. INTRODUCTION

Since non-Newtonian fluids in nature act like elastic solids, flow is prevented by modest shear forces. Casson fluid is one kind of non-Newtonian fluid. The idea was initially developed by Casson in 1959. The hypothesis is based on the interaction of the solid and liquid phases of a two-phase suspension. As prospective Casson fluid possibilities, jam, honey, tomato paste, and extremely concentrated fruit liquids all meet the criteria. Blood from humans is classified as a Casson fluid because it contains numerous Casson fluid-qualifying substances, such as globulin in aqueous base plasma, red blood cells, protein, and fibrinogen. Choi [1] introduced the idea of nanofluid through his investigation of numerous cooling technologies and procedures. These fluids are drawing attention because they offer such an outstanding opportunity for better heat transmission. The blend of Brownian motion and thermophoresis in a nanofluid was initially studied by Buongiorno [2]. Using this framework, Khan and Pop [3] looked at how a nanofluid moves across a stretching sheet in its

boundary layer. Numerous researchers have investigated the stagnation point flow of nanofluids, notably Bachok et al. [6], Ibrahim et al. [5], Mustafa et al. [4], and others. Yacob et al. [7] and Makinde and Aziz [8] also noted challenges with nanofluid flow across a stretching sheet employing a convective boundary condition at the surface. Magnetic nanofluid is a colloidal solution of magnetic nanoparticles and carrier liquid. At the beginning, MHD was tried out on astrophysical and geophysical issues. MHD has received a lot of attention recently due to its applicability in a variety of industries, including engineering and the petroleum industry. Magnetic nanofluids is one of them, and its main goal is to control fluid flow and heat transfer using an external magnetic field. It has been investigated how different geometries of nanofluids react to magnetic fields. Sathies Kumar and Gangadhar [9] hypothesized the effect of a chemical reaction on the slip flow of an MHD Casson fluid over a stretching sheet under the influence of heat and mass transfer. Bhattacharyya [10] examined the effects of thermal radiation on the MHD stagnation point flow using a Casson fluid and a stretching sheet. The unsteady magnetohydrodynamic Casson fluid flow over a vertical cone and flat plate in the presence of a non-uniform heat source was explained by Benazir et al. [11].

Nadeem et al. [12] proposed the MHD 3D Casson fluid flow to pass through a linearly stretched porous sheet. Rizwan et al. [13] investigated the impact of MHD and convective heat transport on a Casson nanofluid passing through a shrinking sheet. Ibrahim and Makinde [14] established a framework for the flow and heat transfer of a Casson nanofluid via a stretching sheet within a magnetohydrodynamic (MHD) stagnation point employing velocity slip and convective boundary conditions. The effects of heat and mass transfer on the MHD flow of Casson fluid that experiences a chemical reaction with suction were examined by Shehzadl et al. [15]. Mukhopadhyay [16] identified the importance of thermal radiation on the flow of a Casson fluid involving heat transfer along a stretching surface in the presence of suction and injection. The Casson nanofluid was proven by Oyelakin et al. [17] on a stretching surface with boundary conditions for radiation of heat, convection, and velocity slip. Although this is not a requirement, all of the aforementioned research are restricted to flows across linearly stretched sheets. For Casson fluid flow and heat transport across a nonlinearly stretched surface, Mukhopadhyay [18] devised a formula. Vajravelu [19] investigated the movement of a viscous fluid over a nonlinearly stretched sheet. We didn't discover how a viscous fluid transmits heat over a nonlinearly stretched sheet until Cortell [20]. The effect of thermal radiation on the flow of an MHD Casson nanofluid on a vertical non-linear stretching surface when Joule heating is present was briefly discussed by Pal et al. [21] using the scaling group approach. Ullah et al.'s study [22] examined how chemical reaction, thermal radiation, heat generation, and convective boundary conditions affected the MHD mixed convection slip flow of Casson fluid through a nonlinearly expanding sheet that surrounded a porous medium. Hayat et al. [23] identified the influence of heat sources and chemical processes on the mixed convection flow of Casson nanofluid over a stretching sheet in the presence of convective boundary conditions. The movement and dispersion of chemically reactive species over a nonlinearly extending sheet in a porous media were studied by Ziabakhsh et al. [24]. Numerous investigations on the boundary layer flow over a non-linear stretched sheet under various heat and mass transfer, slip, and convective boundary conditions, etc. are presented in the literature [25]-[31]. In this study, we investigate the Casson nanofluid's MHD stagnation point flow under the effects of velocity ratio, suction, thermal radiation, viscous dissipation, chemical reaction, Brownian motion, thermophoresis, slip, and convective boundary conditions through a nonlinear stretching sheet. The equations for flow, heat, and mass transfer are solved using the Runge-Kutta-Fehlberg fourth-fifth approach.

2. MATHEMATICAL FORMULATION

Consider a nonlinear stretching sheet that coincides with the plane y=0 and is subject to a steady two-dimensional dissipative MHD stagnation point flow of an incompressible Casson nanofluid. flow being contained in the $y\geq 0$ region. Given that $a>0$, $b>0$, are constants and $n\geq 0$ is the nonlinear stretching parameter, it is assumed that $u=U_w=ax^n$ is the sheet's stretching velocity and $U_\infty=bx^n$ is the free stream velocity.

$U_{slip} = \left(\mu_B + \frac{p_y}{\sqrt{2\pi_c}}\right)\frac{\partial u}{\partial y}$ is used to represent the slip velocity at the surface. A convective heating mechanism, represented by a temperature T_f and a heat transfer coefficient h_f, controls the temperature of the sheet. With $y\rightarrow\infty$, it is believed that C_w is the nanoparticle concentration and that $T\infty$ and $C\infty$ are the ambient temperature and nanoparticle concentration,

respectively. The sheet with constant B_0 is subjected to a perpendicular magnetic field $B(x) = B_0 x^{\frac{n-1}{2}}$.

For an isotropic and incompressible flow of Casson fluid, the rheological equation of state is

$$\tau_{ij} = \begin{cases} 2\left(\mu_B + \frac{p_y}{\sqrt{2\pi}}\right)e_{ij}, & \pi > \pi_c \\ 2\left(\mu_B + \frac{p_y}{\sqrt{2\pi_c}}\right)e_{ij}, & \pi_c > \pi \end{cases}$$

where μ_B is the plastic dynamic

viscosity of the non-Newtonian fluid, p_y is the yield stress of the fluid, π is the product of the component of deformation rate with itself, $\pi=e_{ij}e_{ij}$, e_{ij} is the $(i,j)^{th}$ component of the deformation rate π_c and is the critical value of this product based on the non-Newtonian model.

The equations governing the flow can be expressed as follows

$$\frac{\partial u}{\partial x} + \frac{\partial v}{\partial y} = 0 \quad (1)$$

$$u\frac{\partial u}{\partial x} + v\frac{\partial u}{\partial y} = \nu\left(1+\frac{1}{\beta}\right)\frac{\partial^2 u}{\partial y^2} + U^{\infty}\frac{\partial U_{\infty}}{\partial x} + \frac{\sigma B^2(x)}{\rho_f}(U_{\infty} - u) \quad (2)$$

$$u\frac{\partial T}{\partial x} + v\frac{\partial T}{\partial y} = a\frac{\partial^2 T}{\partial y^2} + \frac{(\rho c)_p}{(\rho c)_f}\left[D_B\frac{\partial C}{\partial y}\frac{\partial T}{\partial y} + \frac{D_T}{T_{\infty}}\left(\frac{\partial T}{\partial y}\right)^2\right] + \frac{\nu}{C_p}\left(1+\frac{1}{\beta}\right)\left(\frac{\partial u}{\partial y}\right)^2 - \frac{1}{(pc)_f}\frac{\partial q_r}{\partial y} \quad (3)$$

$$u\frac{\partial C}{\partial x} + v\frac{\partial C}{\partial y} = D_B\frac{\partial^2 C}{\partial y^2} + \frac{D_T}{T_{\infty}}\frac{\partial^2 T}{\partial y^2} - k_0(C - C_{\infty}) \quad (4)$$

boundary conditions are

$$u = U_w + U_{slip} = ax^n + \left(\mu_B + \frac{p_y}{\sqrt{2\pi_c}}\right)\frac{\partial u}{\partial y}, v = v_w, -k\frac{\partial T}{\partial y} = h_f(T_f - T), C = C_w \text{ at } y = 0\ u \to U_{\infty} = bx^n, v \to 0, T \to T_{\infty}, C \to C_{\infty} \quad (5)$$

In order to turn the partial differential equations into ordinary differential equations, we now introduce the following similarity transformations:

$$\left.\begin{aligned} u = ax^n f'(\xi),\ \xi = y\sqrt{\frac{a(n+1)}{2\nu}}x^{\left(\frac{n-1}{2}\right)},\ v = -\sqrt{\frac{a\nu(n+1)}{2}}x^{\left(\frac{n-1}{2}\right)}\left(f(\xi) + \frac{n-1}{n+1}\xi f'(\xi)\right), \\ \psi = \sqrt{\frac{2a\nu}{(n+1)}}x^{\left(\frac{n+1}{2}\right)}f(\xi),\ \theta(\xi) = \frac{T - T_{\infty}}{T_f - T_{\infty}},\ \varphi(\xi) = \frac{C - C_{\infty}}{C_w - C_{\infty}} \end{aligned}\right\} \quad (6)$$

$$\left(1+\frac{1}{\beta}\right)f''' + ff'' - \frac{2n}{n+1}(f'^2 - A^2) + M(A - f') = 0 \quad (7)$$

$$\left(1+\frac{4}{3}R\right)\ \theta'' + Prf\theta' + PrNb\theta'\varphi' + PrNt\theta'^2 + \left(1+\frac{1}{\beta}\right)PrEcf''^2 = 0 \quad (8)$$

$$\phi'' + Lef\phi' + \frac{Nt}{Nb}\theta'' - Le\gamma\phi = 0 \quad (9)$$

The boundary conditions are

$$f(0) = S, f'(0) = 1 + \delta\left(1+\frac{1}{\beta}\right)f''(0), \theta'(0) = -B_i(1 - \theta(0)), \phi(0) = 1, f'(\infty \to A,\ \ \theta(\infty) \to 0,\ \ \phi(\infty) \to 0, \quad (10)$$

where prime denotes differentiation with respect to ζ..

Non-dimensional skin friction coefficient C_f, local Nusselt number Nu_x and local Sherwood number Sh_x are $C_f = \frac{\tau_w}{\rho U_w^2}$, where $\tau_w = \mu_B\left(1+\frac{1}{\beta}\right)\left(\frac{\partial u}{\partial y}\right)_{y-0}$, $Nu_x = \frac{xq_w}{k(T_f - T_{\infty})}$ and $Sh_x = \frac{xq_m}{k(C_w - C_{\infty})}$, where τ_w is the wall shear stress, q_w and q_m are the heat and mass fluxes at the surface which are defined as:

$$q_w = \left(-\left(k + \frac{16\sigma^* T_{\infty}^3}{3k^*}\right)\left(\frac{\partial T}{\partial y}\right)\right)_{y=0},$$

$$q_m = -D_B\left(\frac{\partial C}{\partial y}\right)_{y=0}$$

Substituting q_w and q_m in the preceding equations, we get

$$Re_x^{1/2}C_f\sqrt{\frac{2}{n+1}} = \left(1+\frac{1}{\beta}\right)f''(0)$$

$$Re_x^{-1/2}Nu_x\sqrt{\frac{2}{n+1}} = -\left(1+\frac{4}{3}R\right)\theta'(0),$$

And

$$\mathrm{Re}_x^{-1/2}\,\mathrm{Sh}_x\sqrt{\frac{2}{n+1}} = -\varphi'(0)$$

where is the local Reynolds number.

3. METHOD OF SOLUTION

The Runge-Kutta-Fehlberg fourth- to fifth-order method along shooting technique is used to solve the nonlinear ordinary differential equations (7) through (9) with boundary conditions (10). First, a system of concurrent ordinary equations is created from a set of non-linear ordinary differential equations of third order in f, second order in g, θ and φ. Runge-Kutta-Fehlberg's fourth-and-fifth technique needs three additional missed initial conditions in order to solve this system. However, when η to infinity, the values of f ′ (η), θ (η),φ (η) are known. Using the shooting technique, these end conditions are utilized to determine the unknown initial conditions at η = 0. By assuming initial conditions, the boundary value problem in the shooting technique is transformed into an initial value problem. The estimated boundary values must match the actual boundary values. One makes an effort to come as close to the boundary value as possible by trial and error or some other scientific method. The selection of the right finite value for the far field boundary condition is the most crucial stage in this procedure. We used the infinity condition at a high but finite value of η, when there are no significant fluctuations in speed, temperature, or other factors. For all possible values of the parameters taken into consideration, we do our bulk computations with the value at η_{max} = 0.6, which is enough to achieve the far field boundary conditions asymptotically.

4. RESULTS AND DISCUSSION

This section focuses on the impact of emerging parameters on velocity, temperature, and concentration, including magnetic (M), nonlinear (n), velocity ratio (A), Casson fluid (β), slip (δ), and suction (S) parameters, as well as Prandtl number (Pr), thermal radiation (R), viscous dissipation (Ec), Brownian motion (Nb), thermophoresis (Nt), Biot number (Bi), Lewis number (Le), and chemical reaction parameters (γ). The fourth-and-fifth approach of Runge-Kutta-Fehlberg is used to solve numerical problems. For numerical findings, we took into account β=0.5, M=0.5, n=1.5, =0.5, A=0.2, δ= 0.1, Pr=0.71, R=0. Nb = 0.1, Nt = 0.1, Ec = 0.1, Bi1 = 0.5, Le = 2.0 and γ=0.5. Unless otherwise noted in the relevant graphs and tables, these values are conserved as common. The distribution of velocity, temperature, and concentration are shown in Figures. 1(a) through 1(c) for different values of the Casson fluid parameter β. It is observed that as β increases, the temperature and concentration distribution increase while the velocity and boundary layer thickness decrease. However, with the growth of the Casson fluid parameter β, the fluid concentration in this case is not much significant.

Figures 2(a) through 2(c) describe the impact of the nonlinear parameter n on velocity, temperature, and concentration curves. It is discovered that as nonlinear parameter values grow, the velocity profile declines while the temperature and concentration profile rise. A magnetic parameter's M influence on velocity distribution is seen in Figure 3. With the magnetic parameter M, the velocity distribution falls. This is because of the Lorentz force that the magnetic field produces.

Figure 4 shows how the suction parameter S affects velocity profiles. With an increase in S, the distributions of velocity slow down. Figure 5 shows how the velocity ratio parameter A affects the velocity field. The velocity is observed to rise with A. Slowing down in the nanofluid's velocity is brought on by an increase in the velocity slip parameter δ. This outcome is shown in Figure 6. Temperature decreases as fluid viscosity increases due to an increase in Prandtl number Pr. In Figure 7, this is depicted.

Figure 8 shows how the radiation parameter R affects temperature. It has been observed that when R increases, so does the temperature. Figure 11 illustrates how Eckert number Ec affects temperature. Because heat is added to the wall through frictional heating, as Ec rises, so does the wall temperature. The presence of the Brownian motion parameter Nb on temperature and concentration profiles is seen in Figures 10(a) and 10(b). With the Brownian motion parameter Nb, temperature rises, but concentration experiences the reverse phenomenon.

Movement of the nanoparticles from the higher temperature region to the lower temperature region in the boundary layer region is caused by an increase in the thermophoresis parameter Nt. Thus, as illustrated in Figures 11(a) and 11(b), increases in Nt imply rises in both the temperature and concentration curves. Figure 12 shows how temperature increases with the Biot number Bi. This is because convective heating and temperature gradient both rise with Bi.

Figures 13 and 14 show, respectively, the effects of the Lewis number Le and the chemical reaction parameter γ on the concentration profiles. It is evident that a rise in Le causes the concentration boundary layer to decrease. Similar results are seen when γ values are raised.

Under restricting circumstances, Tables 1, 2 and 3 show a strong correlation between the current and prior findings.

Table 4 illustrates how different parameters, including γ, R, Nb, Nt, Ec, Bi and γ, affect skin friction coefficient, Nusselt number, and Sherwood number. The table shows that as δ increases, the skin friction coefficient increases.

Sherwood and Nusselt numbers increase with R, and the opposite tendency is seen with δ and Nt. With Nb, Ec and γ Nusselt number decreases but Sherwood number increases.

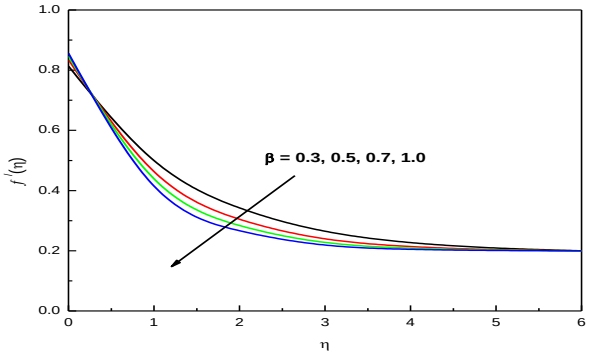

Figure 1 (a): Velocity profiles for various values of β

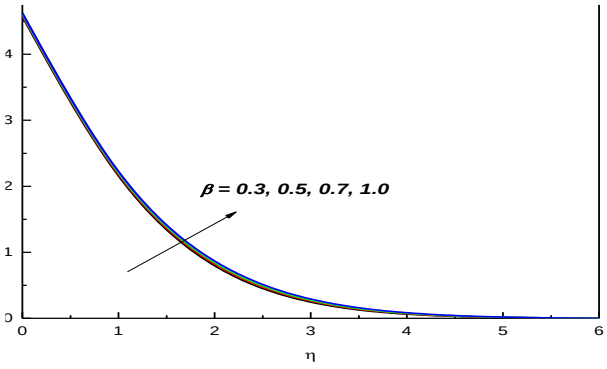

Figure 1(b):Temp profiles for various values of β

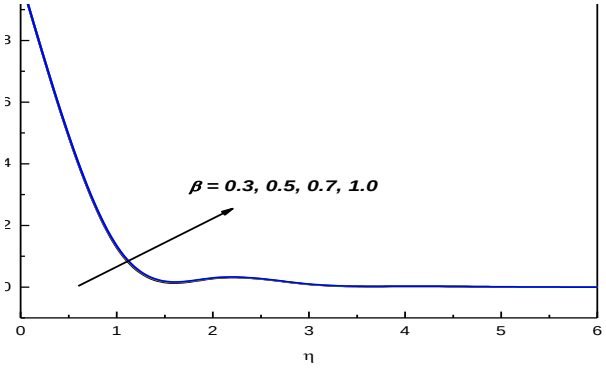

Figure 1(c):Concentration profiles for different values of β

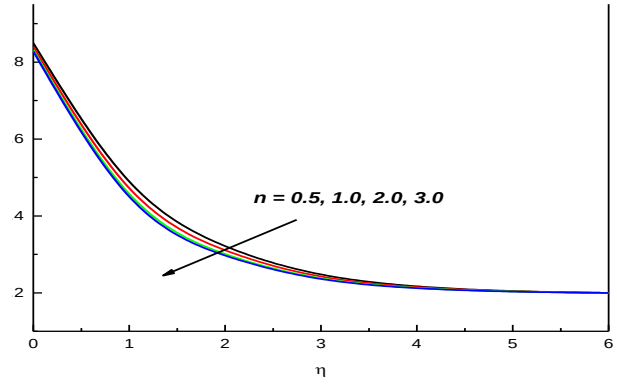

Figure 2 (a): Velocity profiles for various values of n

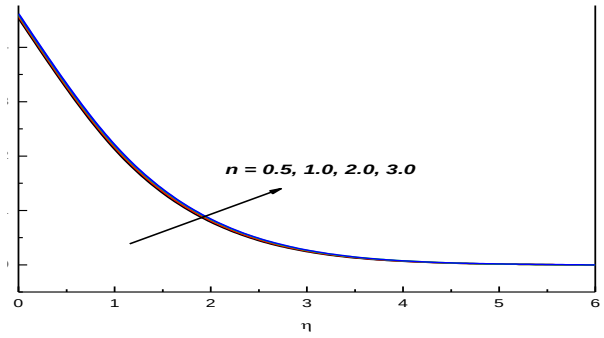

Figure 2(b): Temp. profiles for various values of n

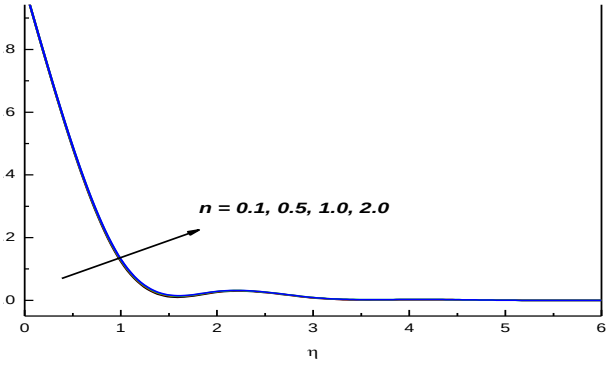

Figure 2(c): Concentration profiles for various values of n

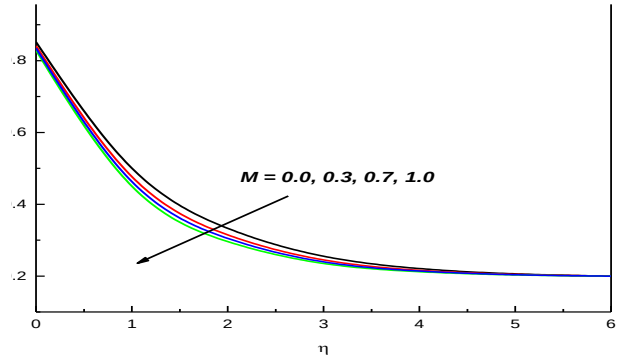

Figure 3: Velocity profiles for various values of M

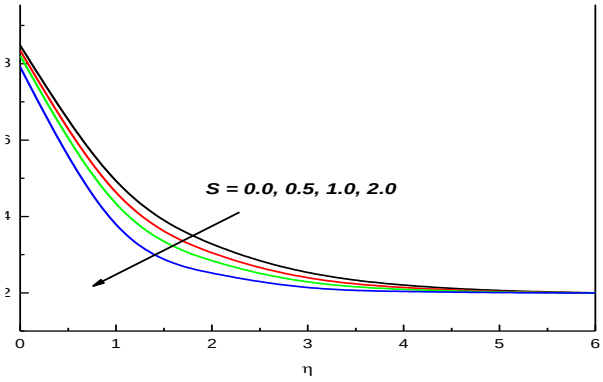

Figure 4. Velocity profiles for different values of S.

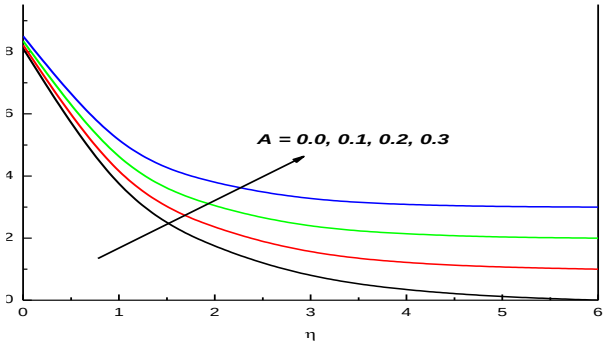

Figure 5. Velocity profiles for various values of A

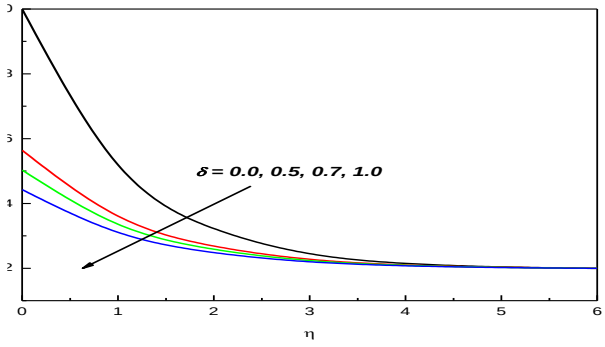

Figure 6. Velocity profiles for various values of δ

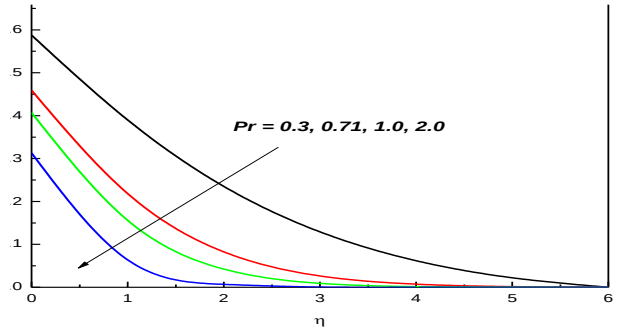

Figure 7. Temp. profiles for various values of Pr

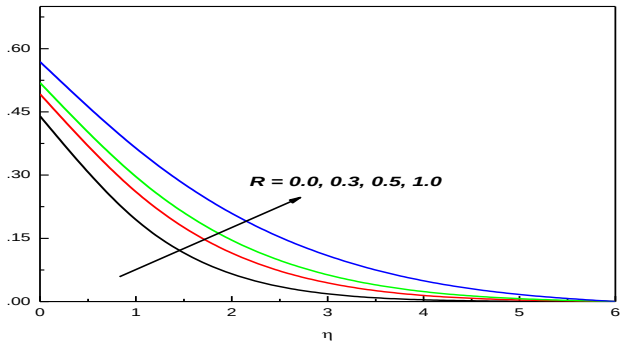

Figure 8. Temperature profiles for various values of R

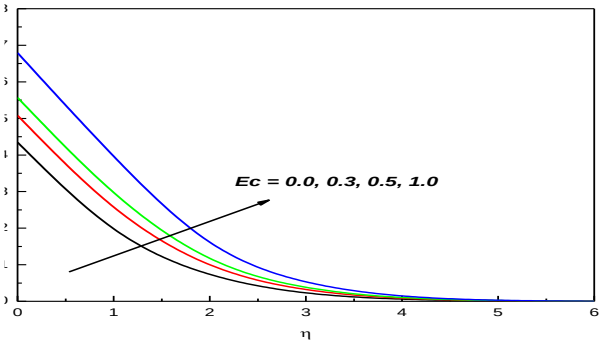

Figure 9. Temperature profiles for different values of Ec

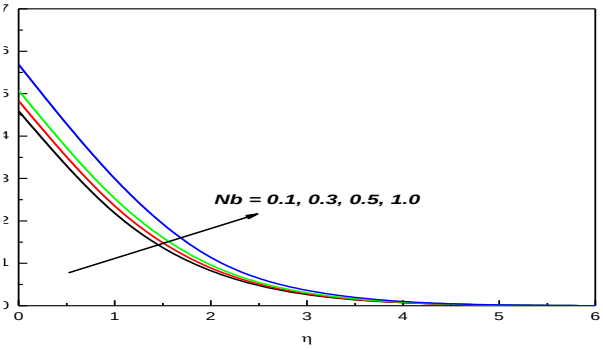

Figure 10(a). Temperature profiles for various values of Nb

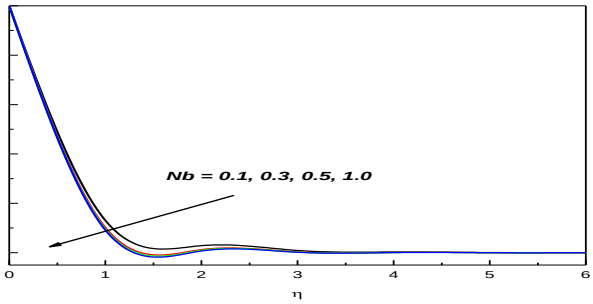

Figure 10 (b). Concentration profiles for different values of Nb

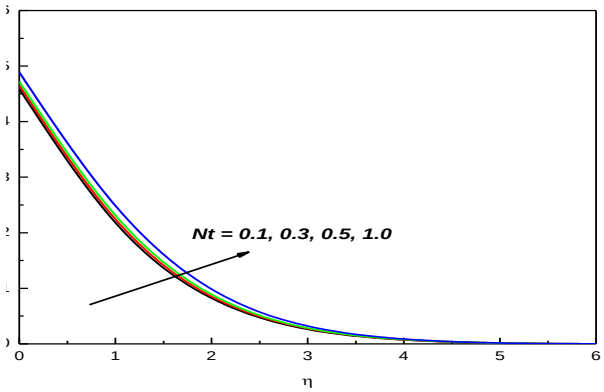

Figure 11(a). Temp. profiles for various vales of Nt

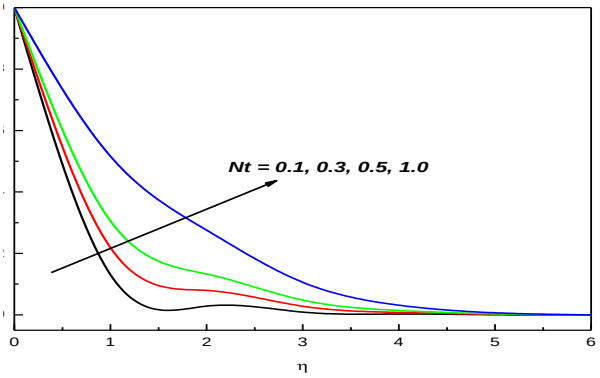

Figure 11(b). Concentration profiles for various values of Nt

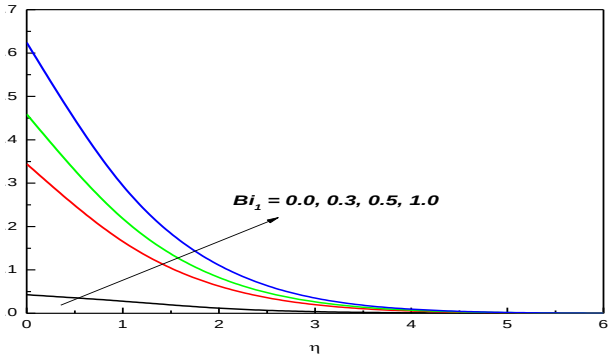

Figure 12: Temp. profiles for various values of Bi1

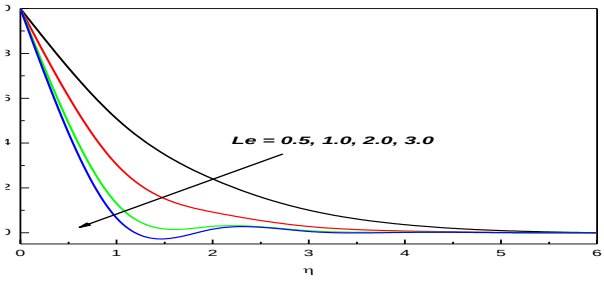

Figure 13.Concentration profiles for various values of Le

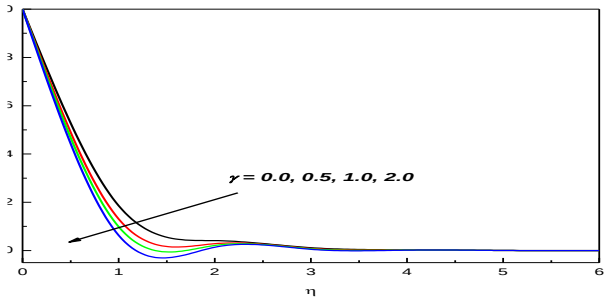

Figure 14: Concentration profiles for various values of γ

Table 1 Comparison of the skin friction coefficient at M=0, δ=0.0, S=0.0 and n=0.1 for β various values of and A

β	A	**Mondal et al. [36]**	**Present**
1	0.0	-1.41421	-1.41422
5	0.0	-1.09544	-1.09543
1000	0.01	-0.99782	-0.99804
1000	0.1	-0.96937	-0.96936
1000	0.2	-0.91811	-0.91815

Table 2 Comparison of -f``(0) at M-0, A=0.0, β=1000, S=0.0 and n=1.0 for various values of δ

δ	**Ibrahim and Makinde [14]**	**Oyelakin et al. [32]**	**Present**
0.0	1.0000	1.000000	1.00000
0.1	0.8721	0.872083	0.87202
0.2	0.7764	0.776377	0.77633
0.5	0.5912	0.591195	0.59122
1.0	--	0.430160	0.43013
2.0	0.2840	0.283979	0.28395
3.0	--	0.214054	0.21402
5.0	0.1448	0.144714	0.14481
10.0	0.0812	0.080932	0.08128

Table 3. Comparison of -θ`(0) and -ϕ`(0) when M=β=A=S=R=Ec=Q=γ=0.0, Bi=1000, and β→∞

n	Nt	Rana and Bhargava [33]		Mabood and Khan [34]		Present	
		-θ′(0)	-ϕ′(0)	-θ′(0)	-ϕ′(0)	-θ′(0)	-ϕ′(0)
0.2	0.3	0.4533	0.8395	0.4520	0.8402	0.45191	0.84015
	0.5	0.3999	0.8048	0.3987	0.8059	0.39902	0.80576
3.0	0.3	0.4282	0.7785	0.4271	0.7791	0.42724	0.77913
	0.5	0.3786	0.8323	0.3775	0.7390	0.37771	0.73871
10	0.3	0.4277	0.7654	0.4216	0.7660	0.42183	0.76594
	0.5	0.3739	0.7238	0.3728	0.7248	0.37304	0.72432

Table 4. Numerical values of skin friction coefficient $-\left(1+\frac{1}{\beta}\right)f''(0)$, Nusselt number $-\left(1+\frac{4}{3}R\right)\theta'(0)$ and Sherwood number $-\phi'(0)$ for different values of $\delta, R, Nb, Nt, Ec, Q, Bi, \gamma$

δ	R	Nb	Nt	Ec	Q	Bi	γ	$-\left(1+\frac{1}{\beta}\right)f''(0)$	$-\left(1+\frac{4}{3}R\right)\theta'(0)$	$\phi'(0)$
0.2	0.2	0.3	0.3	0.2	0.2	0.6	0.3	-1.69741	0.33293	0.77276
0.7								-0.95336	0.3319	0.72177
1.5								-0.61222	0.32882	0.69753
	0.7							--	0.42881	0.81314
	1.0							--	0.46961	0.82833
		0.7						--	0.31792	0.9049
		1.0						--	0.29133	0.94925
			0.5					--	0.33176	0.67007
			0.7					--	0.32924	0.46865
				0.7				--	0.27544	0.83875
				1.5				--	0.20313	0.92165
					-0.3			--	0.35713	0.74645
					0.3			--	0.34223	0.76274
						0.5		--	0.09662	0.92604
						1.0		--	0.60922	0.59413
							0.0	--	0.33343	0.65633
							0.3	--	0.33234	0.91964

REFERENCES

[1] S. U. S. Choi, Enhancing thermal conductivity of fluids with nanoparticles, The Proceedings of the 1995 ASME International Mechanical Engineering Congress and Exposition, San Francisco, CA, ASME, FED, 231, 99-105, 1995.

[2] J. Buongiorno, Convective transport in nanofluids, Journal of Heat Transfer, 128, 240-250, 2006.

[3] W. A. Khan and I. Pop, Boundary-layer flow of a nanofluid past a stretching sheet, International Journal of Heat and Mass Transfer, 53, 2477-2483, 2010.

[4] M. Mustafa, T. Hayat, I. Pop, S. Asghar and S. Obaidat, Stagnation-point flow of a nanofluid towards a stretching sheet, International Journal of Heat and Mass Transfer, 54, 5588-5594, 2011.

[5] W. Ibrahim, B. Shankar and M. M. Nandeppanavar, MHD stagnation point flow and heat transfer due to nanofluid towards a stretching sheet, International Journal of Heat and Mass Transfer, 56, 1-9, 2013.

[6] N. Bachok, A. Ishak and I. Pop, Stagnation-point flow over a stretching/shrinking sheet in a nanofluid, Nanoscale Research Letters, 6, 1-10, 2013.

[7] N. A. Yacob, A. Ishak, I. Pop and K. Vajavelu,

Boundary layer flow past a stretching/shrinking surface beneath an external uniform shear flow with a convective surface boundary condition in a nanofluid, Nanaoscale Research Letters, 6, 1-7, 2011.

[8] O. D. Makinde and A. Aziz, Boundary layer flow of a nanofluid past a stretching sheet with a convective boundary conditions, International Journal of Thermal Sciences, 50, 1326-1332, 2011.

[9] P. Sathies Kumar and K. Gangadhar., Effect of chemical reaction on slip flow of MHD Casson fluid over a stretching sheet with heat and mass transfer, Advances in Applied Science Research, 2015, 6(8):205-223.

[10] K Bhattacharyya, MHD stagnation point flow of Casson fluid and heat transfer over a stretching sheet with thermal radiation, Journal of Thermodynamics, Volume 2013 (2013), Article ID 169674, 9 pages.

[11] Benazir J., Sivaraj A, Makinde OD. Unsteady magnetohydrodynamic Casson fluid flow over a vertical cone and flat plate with non-uniform heat source/sink. Int J Eng Res Africa. 2016;21: 69–83.

[12] Nadeem S, Haq RU, Akbar NS, Khan ZH. MHD three-dimensional Casson fluid flow past a porous linearly stretching sheet. Alexandria Eng J. Faculty of Engineering, Alexandria University; 2013;52: 577–582. doi: 10.1016/j.aej.2013.08.005.

[13] U.H. Rizwan, S. Nadeem, Z.H. Khan, T.G. Okedayo, Convective heat transfer and MHD effects on Casson naofluid flow over a shrinking sheet,Cent. Eur. J. Phys, 12 (12) (2014), pp. 862–871.

[14] W. Ibrahim and O. D. Makinde, Magnetohydrodynamic stagnation point flow and heat transfer of Casson nanofluid past a stretching sheet with slip and convective boundary conditions, Journal of Aerospace Engineering, 29, 1-11, 2016. (Base Paper)

[15] S. A. Shehzadl, T. Hayat, M. Qasim and S. Asghar, Effects of mass transfer on MHD flow of Casson fluid with chemical reaction and suction, Brazilian journal of chemical engineering, 30 (1), 187-195 (2013).

[16] Mukhopadhyay S. Effects of thermal radiation on Casson fluid flow and heat transfer over an unsteady stretching surface subjected to suction/blowing. Chinese Phys B. 2013;22: 114702. doi: 10.1088/1674-1056/22/11/114702.

[17] I. S. Oyelakin, S. Mondal and P. Sibanda, Unsteady Casson nanofluid flow over a stretching sheet with thermal radiation, convective and slip boundary conditions, Alexandria Engineering Journal, 55, 1025-1035, 2016.

[18] Mukhopadhyay, S., Casson fluid flow and heat transfer over a nonlinearly stretching surface, Chin. Phys. B, 22 (2013), 7, pp. 074701, DOI: 10.1088/1674-1056/22/7/074701

[19] Vajravelu, K. (2001) Viscous Flow over a Nonlinearly Stretching Sheet. Applied Mathematics and Computation, 124, 281-288

[20] Cortell, R. (2007) Viscous Flow and Heat Transfer over a Nonlinearly Stretching Sheet. Applied Mathematics and Computation, 184, 864-873. http://dx.doi.org/10.1016/j.amc.2006.06.077

[21] D Pal., N Roy., K Vajravelu, Effects of thermal radiation and Ohmic dissipation on MHD Casson nanofluid flow over a vertical non-linear stretching surface using scaling group, International Journal of Mechanical Sciences 114 (2016) 257–267.

[22] Ullah I, Bhattacharyya K, Shafie S, Khan I (2016) Unsteady MHD Mixed Convection Slip Flow of Casson Fluid over Nonlinearly Stretching Sheet Embedded in a Porous Medium with Chemical Reaction, Thermal Radiation, Heat Generation/Absorption and Convective Boundary Conditions. PLoS ONE 11(10): e0165348. doi:10.1371/journal.pone.0165348

[23] T. Hayat, M. Bilal Ashraf, S. A. Shehzad and A. Alsaedi, Mixed Convection Flow of Casson Nanofluid over a Stretching Sheet with Convectively Heated Chemical Reaction and Heat Source/Sink, Journal of Applied Fluid Mechanics, Vol. 8, No. 4, pp. 803-813, 2015.

[24] Ziabakhsh, Z., Domairry, G., Bararnia, H. and Babazadeh, H., Analytical solution of flow and diffusion of chemically reactive species over a nonlinearly stretching sheet immersed in a porous medium. J. Taiwan Institute Chemical Eng., 41, p. 22 (2010).

[25] Abbas, Z. and Hayat, T. (2011) Stagnation Slip Flow and Heat Transfer over a Nonlinear Stretching Sheet. Numerical Methods for Partial Differential Equations, 27, 302-314.

[26] Hayat, T., Javed, T. and Abbas, Z. (2009) MHD Flow of a Micropolar Fluid near a Stagnation-Point Towards a Non-Linear Stretching Surface. Nonlinear Analysis: Real World Applications, 10, 1514-1526

[27] Mabood, F., Khan, W.A. and Ismail, A.I.M. (2015) MHD Boundary Layer Flow and Heat Transfer of Nanofluids over a Nonlinear Stretching Sheet: A Numerical Study. Journal of Magnetism and Magnetic Materials, 374, 569-576.

[28] Prasad, K.V., Vajravelu, K. and Dattri, P.S. (2010) Mixed Convection Heat Transfer over a Non-Linear Stretching surface with Variable Fluid Properties.

International Journal of Non-Linear Mechanics, 45, 320-330. http://dx.doi.org/10.1016/j.ijnonlinmec.2009.12.003

[29] Rana, P. and Bhargava, R. (2012) Flow and Heat Transfer of a Nanofluid over a Nonlinearly Stretching Sheet: A Numerical Study. Communications in Nonlinear Science and Numerical Simulation, 17, 212-226. http://dx.doi.org/10.1016/j.cnsns.2011.05.009

[30] Ghotbi, A.R. (2009) Homotopy Analysis Method for Solving the MHD flow over a Non-Linear Stretching Sheet. Communications in Nonlinear Science and Numerical Simulation, 14, 2653-2663. http://dx.doi.org/10.1016/j.cnsns.2008.08.006

[31] Fanga, T. (2014) Magneto-Hydrodynamic Viscous Flow over a Nonlinearly Moving Surface: Closed-Form Solutions. The European Physical Journal Plus, 129, 92. http://dx.doi.org/10.1140/epjp/i2014-14092-4.

[32] I. S. Oyelakin, S. Mondal and P. Sibanda, Unsteady Casson nanofluid flow over a stretching sheet with thermal radiation, convective and slip boundary conditions, Alexandria Engineering Journal, 55, 1025-1035, 2016.

[33] P. Rana and R. Bhargava, Flow and heat transfer of a nanofluid over a nonlinearly stretching sheet: A numerical study, Communications in Nonlinear Science and Numerical Simulation, 17, 212-226, 2012.

[34] F. Mabood, W. A. Khan and A. I. M. Ismail, MHD boundary layer flow and heat transfer of nanofluids over a nonlinear stretching sheet: A numerical study, Journal of Magnetism and Magnetic Materials, 374, 569-576, 2015.